Sonochemical preparation of lead sulfide nanocrystals in an oil-in-water microemulsion

Hui Wang, Jian-Rong Zhang, Jun-Jie Zhu*

Key State Laboratory of Coordination Chemistry, Laboratory of Mesoscopic Materials Science, Department of Chemistry, Nanjing University, Nanjing 210093, People's Republic of China

Abstract

Lead sulfide (PbS) nanocrystals have been successfully prepared in an oil-in-water microemulsion by a sonochemical method. The product is characterized by using techniques such as X-ray powder diffraction, transmission electron microscopy, X-ray photoelectron spectroscopy, and energy-dispersive X-ray analysis. The as-prepared PbS nanocrystals crystalize in a cubic structure and have an average crystal size of ca. 11 nm. The product is composed of uniform spherical nanoparticles with narrow size distribution and high purity. A probable mechanism for the formation of nanocrystalline PbS particles in a toluene-in-water microemulsion with the inducement of ultrasound irradiation is proposed.
© 2002 Elsevier Science B.V. All rights reserved.

1. Introduction

Semiconductor nanocrystals have electronic properties intermediate between those of molecular entities and macrocrystalline solids and are at present the subject of intense research [1–4]. In the past decade, there has been much interest in the synthesis and physical characterizations of nanoscale sulfide semiconductive materials. Various new methods for the preparation of sulfide nanocrystals have been reported in recent years such as employing ultraviolet irradiation [5], γ-ray irradiation [6,7], the solvothermal method [8–10], microwave assisted heating [11–13], chemical bath deposition [14], electrodeposition [15–17], the sonoelectrochemical method [18], and so on. It is worth mentioning that using microemulsions and ultrasound irradiation are two synthetic methods for nanosized sulfides that have been studied intensively and arousing more and more attention.

Microemulsions have been intensively used as spatially constrained microreactors for the controlled growth of inorganic materials [19–21]. In the case of a microemulsion, the reactions take

---

*Corresponding author. Tel.: +86-25-331-7761; fax: +86-25-3594976.

E-mail address: jjzhu@nju.edu.cn (J.-J. Zhu).

place in the core of the microemulsions and the hydrophilic head groups of the surfactant molecules. Surfactants provide several types of well-organized assemblies which provide specific sites, geometrical control and stabilization to particulate assemblies formed within the organized surfactant assemblies. Sulfide nanoparticles such as CdS, ZnS, CuS, PbS, have been successfully prepared by this method [22–25] and have been well characterized and studied.

Currently, ultrasound irradiation has become an important tool in chemistry. It provides an unusual mechanism for generating high-energy chemistry with extremely high local temperatures and pressures and an extraordinary heating and cooling rate. Sonochemistry drives principally from acoustic cavitation: the formation, growth, and implosive collapse of bubbles in liquids [26]. When solutions are exposed to strong ultrasound irradiation, bubbles are implosively collapsed by acoustic fields in the solution. High-temperature and high-pressure fields are produced at the centers of the bubbles. The implosive collapse of the bubbles generates a localized hotspot through adiabatic compression or shock wave formation within the gas phase of the collapsing bubbles. The conditions formed in these hotspots have been experimentally determined, with the transient temperature of ~ 5000 K, pressure of > 1800 atm and cooling rates in excess of 10^{10} K/s [27]. These extreme conditions formed during ultrasound irradiation have already been applied to prepare some nanophasic sulfides. For example, Suslick and his co-workers have sonicated a slurry of molybdenum hexacarbonyl and sulfur in an isodurene solution and obtained MoS_2 [28]. Gedanken's group synthesized ZnS coated on silica microspheres by sonicating a slurry of silica microspheres, thioacetamide and zinc acetate [29]. Similarly, as described in one of their earlier publications [30], ultrasonic irradiation of a slurry of silica microspheres, cadmium sulfate, and thiourea in an aqueous medium for 3 h would yield cadmium sulfide–silica composite. Gedanken and co-workers have also successfully established sonochemical methods for the fabrication of a variety of nanocrystalline metal sulfides such as HgS and PbS nanoparticles [31], Ag_2S/PVA and

CuS/PVA nanocomposite [32], $RuS_{1.7}$ [33] and In_2S_3 [34] nanoparticles. The sonochemical formation of CdS nanoparticles in aqueous solutions [35,36] and in CS_2–water–ethylenediamine system [37] have also been recently reported.

PbS is a typical narrow band gap semiconductor. It is one of the most attractive metal sulfides for a wide variety of applications, such as Pb^{2+} ion-selective sensors and IR detectors [31]. Various processes, including sintering precipitation, vacuum evaporation, and electrochemical deposition have been employed to produce PbS bulk material or PbS films [38–40]. In this paper, we report on a sonochemical method for the preparation of PbS nanocrystals in an oil-in-water microemulsion. Sulfur–toluene solution (STS) was chosen as the sulfur source. When STS was mixed with water in the presence of sodium lauryl sulfate (SLS) as the surfactant, a liquid–liquid heterogeneous system was formed. The cavitation behavior of ultrasound irradiation can lead to extraction, mixed phase reactions and emulsification in such a liquid–liquid heterogeneous system. Thus, an o/w microemulsion of toluene-in-water can be formed under ultrasound irradiation. This synthetic design was motivated by the known simple interaction between sulfur and ethylenediamine, but it provides special conditions for the formation and growth of the PbS nanocrystals in such a microemulsion system in the presence of high-intensity ultrasound irradiation.

2. Experimental section

All the reagents were of analytical purity, and were used without further purification. Lead acetate $(Pb(Ac)_2 \cdot 2H_2O)$ was purchased from Shanghai Chemical Reagent Factory (China). Ethylenediamine (en) and SLS were purchased from Nanjing Chemical Reagent Factory (China). Absolute ethanol and acetone were purchased from Beijing Chemical Reagent Factory (China). Distilled water was used throughout the experiments.

In a typical procedure, 5 ml STS was mixed with 95 ml aqueous solution containing 0.005 mol $Pb(Ac)_2$, 0.4 g SLS and 5 ml ethylenediamine.

STS was prepared by stirring 1.0 g sulfur powders in 50 ml toluene at about 313 K till the sulfur powder was completely dissolved. Then the mixture was exposed to ultrasound irradiation under ambient air for 30 min. Ultrasound irradiation was accomplished with a high-intensity ultrasound probe (Xinzhi Co., China; JY92-2D; 0.6 cm-diameter; Ti-horn, 20 kHz, 60 W/cm^2) immersed directly in the reaction solution. The sonication was conducted without cooling so that a temperature of about 333 K was reached at the end of the reaction. When the reaction finished, a black precipitate occurred. The precipitate was separated by centrifugation, washed with distilled water, absolute ethanol and acetone in sequence, and dried in air at room temperature for 8 h. The products are characterized by using techniques such as X-ray powder diffraction (XPRD), transmission electron microscopy (TEM), X-ray photoelectron spectroscopy (XPS), energy-dispersive X-ray analysis (EDAX).

The XPRD analysis was performed by Shimadzu XD-3A X-ray diffractometer at a scanning rate of 4°/min in the 2θ range from 20° to 60°, with graphite monochromatized Cu Kα radiation ($\lambda = 0.15418$ nm). TEM measurements were carried out by employing JEOL JEM-200CX TEM, using an accelerating voltage of 200 kV. The samples used for TEM observations were prepared by dispersing some products in ethanol followed by ultrasonic vibration for 30 min, then placing a drop of the dispersion onto a copper grid coated with a layer of amorphous carbon. The surface of the product was detected by X-ray photoelectron spectra recorded on ESCALAB MK II X-ray photoelectron spectrometer, using non-monochromatized Mg Kα X-ray as the excitation source and choosing C1s (284.6 eV) as the reference line. EDAX measurements were performed on the PV9100 instrument.

3. Results and discussions

The XPRD pattern of the as-prepared PbS nanoparticles (Fig. 1) shows the presence of broad peaks corresponding to the cubic crystal structure. The positions and intensities of the peaks are in
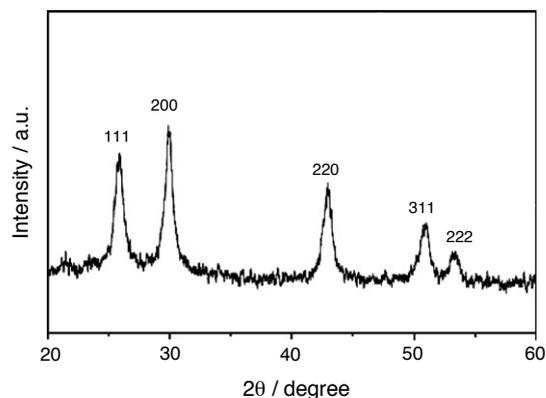

Fig. 1. XPRD pattern of the as-prepared PbS nanocrystals.

good agreement with the literature values for cubic phase PbS with a zinc blende structure.[1] The broadening of the peaks indicates that the crystal sizes are very small. The average size of the as-prepared PbS nanocrystals are estimated to 11 nm according to the Debye–Scherrer formula [41].

The dimensions and morphologies of the PbS nanocrystals are shown in the TEM image (Fig. 2a). It is apparent that the as-prepared PbS nanocrystals present uniform spherical morphologies and their sizes are in the range of 8–13 nm, which is in good accordance with the results calculated according to the XPRD pattern. The particle size distribution, measured directly from the TEM image is shown as histograms in Fig. 2b.

The product is also characterized by XPS and EDAX for the evaluation of their composition and purity. The wide scanning XPS spectrum of the as-prepared PbS nanocrystals is shown in Fig. 3. The C1s peaks should be corrected to 284.6 eV and all the other peaks should be corrected accordingly. The binding energies obtained from XPS analysis show good agreement with the literature [42]. No peaks of impurities such as Pb(0), Pb (IV) or N are observed in the spectrum, indicating the high purity of the product. Figs. 4a and b show the high-resolution XPS spectra of Pb (4f) and S (2p), respectively. Peak areas of Pb (4f) and S (2p) cores are measured and quantification of the peaks gives

---

[1] Joint Committee on Powder Diffraction Standards (JCPDS), File No 5-0592.
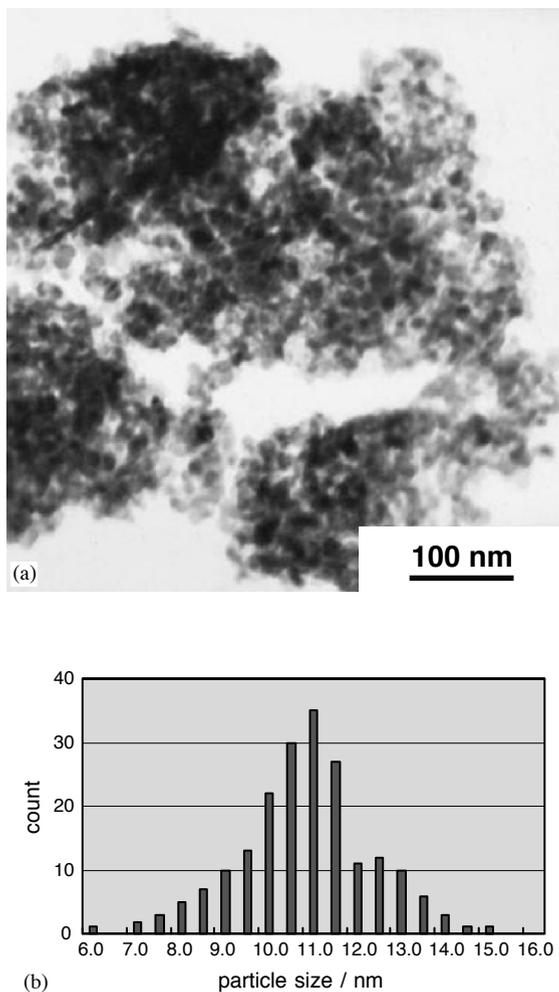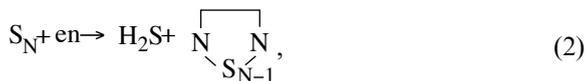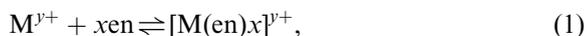
(a)

100 nm

(b)

Fig. 2. (a) TEM image of the as-prepared PbS nanocrystals; and (b) particle size distribution picture obtained by direct measurements in the TEM image.

the ratio of Pb:S to be 1.19:1, which indicates that the surface of the sample is rich in Pb. XPS primarily monitors concentrations at the surface of the examined samples, which may not be representative of the sample as a whole. The deviation of atomic ratio of Pb:S to the expcted 1:1 may be attributed to the excessive Pb^{2+} absorbed on the surface of PbS nanocrystals. The results of EDAX measurement reveal that the as-prepared PbS nanocrystals are of high purity and the average atomic ratio of Pb:S is 53.6:46.4, which also points out that the surface of the product is

rich in Pb. The results are consistent with the XPS results.

The formation of nanocrystalline lead sulfide is based on the known interaction between sulfur and ethylenediamine. Lelieui [43] and Parkin [44,45] have developed a room temperature liquid-amine route to metal chalcogenides based on the reactions of sulfur, selenium or tellurium with elemental metals in liquid ammonia in a pressure vessel. They pointed out that in sulfur–ammonia solutions, there were various sulfur imido anions (S_2N^-, S_3N^-, S_4N^-) as well as sulfur polyaniones (S_6^-, S_4^-) and zero oxidation sulfur species ($S_xNH_3^-$, $x = 1-8$). Sulfur could also dissolve in organo-amine to produce colored N,N′-diamine–polysulfide solution and hydrosulfuric acid [46]. Ethylenediamine plays an important role in generating the active sulfur species, such as S^{2-}. Meanwhile, ethylenediamine as a strong bidenate ligand can co-ordinate with metal ions to give stable complexes in the form of chelate compounds $[M(en)x]^{y+}$. These chelate compounds would then react with the active sulfur species, leading to the formation of metal sulfides. The whole process can be described as below

$$M^{y+} + x\text{en} \rightleftharpoons [M(en)x]^{y+}, \qquad (1)$$

$$S_N + \text{en} \rightarrow H_2S + \underset{S_{N-1}}{N \quad N}, \qquad (2)$$

$$yH_2S + 2[M(en)x]^{y+} \rightarrow M_2S_y + 2x\text{en} + 2yH^+. \qquad (3)$$

The nature and morphology of the metal sulfides via such liquid-ammonia route greatly depend on the preparation conditions. When the reactions of a range of transition metals and main metals with sulfur–liquid ammonia solutions were carried out at room temperature in Telflon-in glass Younges-type pressure tubes, the as-prepared metal sulfides were mainly amorphous or poorly crystalline [45]. If such reactions were carried out under solvothermal conditions, nanocrystalline metal sulfides with different morphologies could be obtained [9,47]. Gedanken et al. [31] employed ultrasound irradiation to induce such liquid-ammonia reactions in ethylenediamine and managed to get nanocrystalline spherical HgS and rectangular PbS particles. In the present work, we
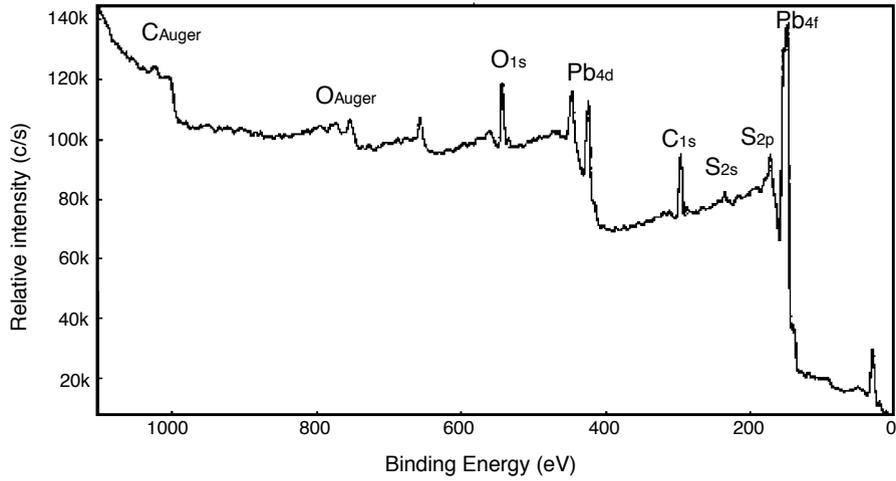
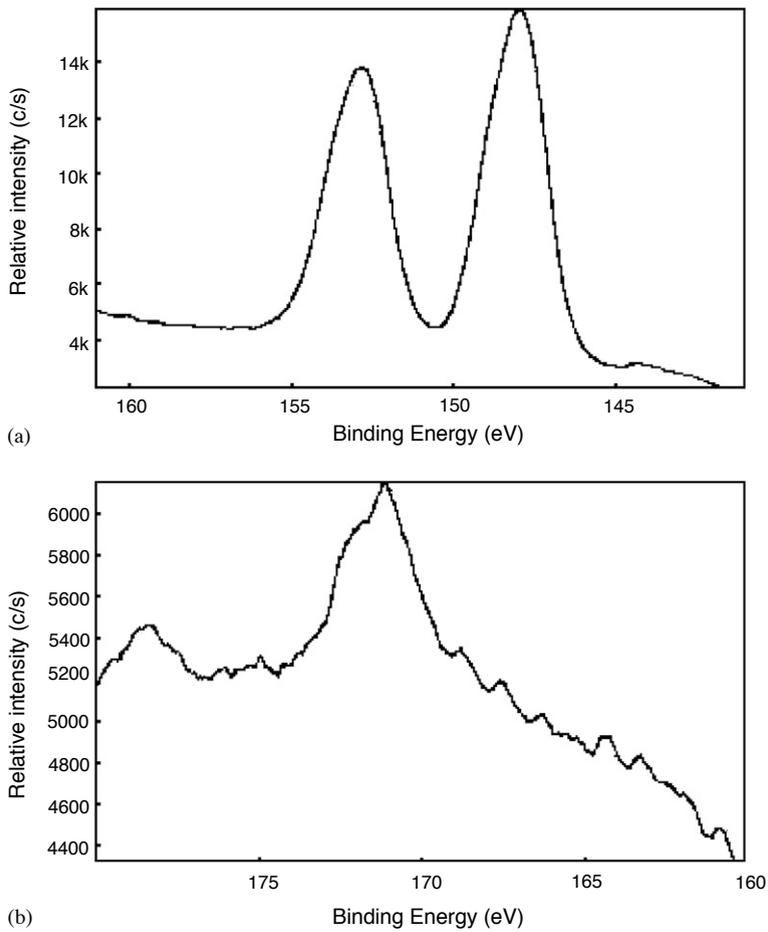Fig. 3. The wide XPS spectrum of the as-prepared PbS nanocrystals.

Fig. 4. High-resolution XPS spectra of the as-prepared PbS nanocrystals: (a) Pb (4f); and (b) S (2p).

design an ultrasound-induced microemulsion route to prepare lead sulfide nanocrystals based on the reactions described above. The schematic presentation of formation of lead sulfide nanocrystals is shown in Fig. 5.

In the toluene–water heterogeneous system, sulfur powder was dissolved in toluene, the oil phase, and $[Pb(en)x]^{2+}$ and excessive ethylenediamine was in the water phase. No reaction took place at this stage. After SLS was added and the mixture was irradiated with high-intensity ultrasound for a period of time, toluene droplets were homogenized and sulfur began to react with ethylenediamine at the oil–water interface to give H_2S. SLS played a critical role in this process. It not only promoted the formation of the microemulsion as the oil droplet stabilizer, but also provided the sites for the reactions by bridging the oil–water interface. Then the released H_2S combined with $[Pb(en)x]^{2+}$ to form PbS nuclei in the water phase. These freshly generated nuclei were unstable and have the tendency to grow into larger grains.

In the process of the formation of PbS nanocrystals, the ultrasound irradiation plays an important role. Sulfur can react with ethylenediamine at room temperature. However, it was found that in this system the reactions did not take place without the inducement of ultrasound irradiation, because sulfur and ethylenediamine existed in different phases, which restrained the reactions. Ultrasound waves that are intense enough to produce cavitation can drive chemical reactions such as oxidation, reduction, dissolution and decomposition [27,48]. Other reactions driven by high-intensity ultrasound irradiation such as promotion of polymerization have also been reported to be induced by ultrasound. Ultrasound irradiation differs from traditional energy sources (such as heat, light or ionizing radiation) in duration, pressure and energy per molecule. It has been known that during the sonochemical process, three different regions [48] are formed: (a) the inner environment (gas phase) of the collapsing bubbles, where the elevated temperatures and pressures are produced; (b) the interfacial region between the cavitation bubbles and the bulk solution where the temperature is lower than in the gas-phase region but still high enough to induce a sonochemical reaction; (c) the bulk solution, which is at ambient temperature. Among the three regions mentioned above, it appears that the current sonochemical reactions occur within the interfacial region, yielding nanoparticles, because of the very high quenching rate experienced by the products. The critical temperature of ethylenediamine (591 K) is lower than that of water (647 K), so the velocity of the diffusion of ions and the interparticle collisions in ethylenediamine under ultrasound irradiation will be more rapidly due to its lower viscosity. When the bubbles collapse, the ethylenediamine in the water phase will be vaporized. These vaporized ethylenediamine molecules react with the sulfur dissolved in the toluene droplets via the connection of SLS which acts as the bridge over the oil–water interface, leading to the formation of the released H_2S. Moreover, ultrasound irradiation also affects the growth of the nanoparticles. Once the nuclei of
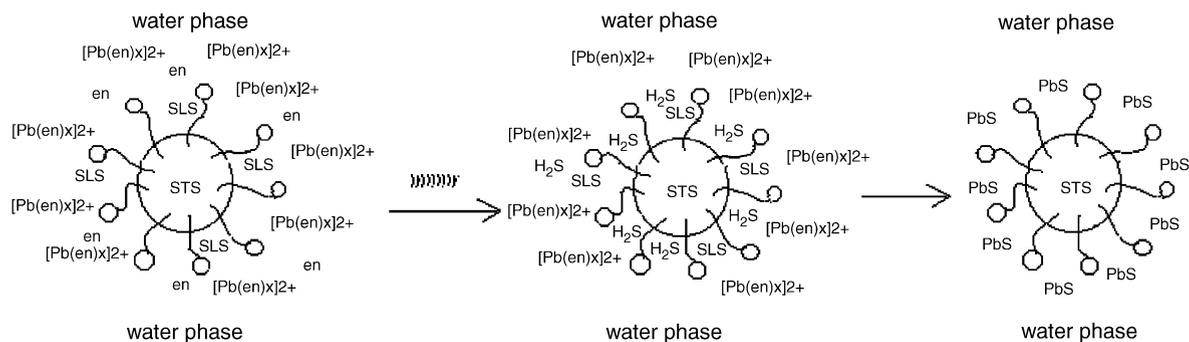

Fig. 5. The schematic presentation of sonochemical formation of PbS nanocrystals in o/w microemulsion.

PbS formed, they were unstable and have the a tendency to grow into larger grains. The increase of the grain size with sonication time can be explained by the effect of acoustic cavitation on PbS. The implosive collapse of a cavity on an extended solid surface in a liquid has been recognized to be different from the symmetrical implosion of cavities observed in homogeneous, pure liquids [49]. In the former case, asymmetric implosion results in the formation of high-speed microjets of liquids as well as shock waves that drive the solid particles to high velocities, which leads to interparticle collisions. The collisions between the PbS particles at high velocities result in increased local heating and condensation to form larger particles [50]. The increase in size of the PbS nanoparticles can also involve the crystal growth process. When the PbS nanoparticles formed, smaller particles had a large number of dangling bonds, defect sites, or traps [51]. During the reaction time, the surface states changed. Dangling bonds, defect sites or traps will decrease gradually, and the grains will grow. After a period of time under ultrasound irradiation, the surface states become stable, and the size of the grains cease to increase any more. In our experiments, 30 min was chosen as the sonication time. When the sonication time decreased to less than 20 min, the reactions was not completed. If the reaction time was prolonged to 1 h, the size and morphology of the products almost remained unchanged. Therefore, we may draw the conclusion that sonication for 30 min is suitable for both the nucleation and the growth of the PbS nanoparticles.

4. Conclusions

In summary, a novel sonochemical method for the preparation of PbS nanocrystals in oil-in-water microemulsions has been established. The products have uniform shape, narrow size distributions and high purity. The probable mechanism for the formation of nanocrystalline lead sulfide particles in a toluene–SLS–water microemulsion induced by ultrasound irradiation is proposed. We can foresee the extension of this method to the preparation of other nanocrystalline metal sulfides.

References

[1] D. Dounghong, J. Ramsden, M. Gratzel, J. Am. Chem. Soc. 104 (1982) 29777.
[2] Y. Wang, N. Herron, J. Phys. Chem. 95 (1991) 525.
[3] A. Henglein, Chem. Rev. 89 (1989) 1861.
[4] H. Weller, Adv. Mater. 5 (1993) 88.
[5] C.Y. Wang, X. Mo, Y. Zhou, Y.R. Zhu, H.T. Liu, Z.Y. Chen, J. Mater. Chem. 10 (2000) 607.
[6] X.C. Jiang, Y. Xie, J. Lu, L.Y. Zhu, W. He, Y.T. Qian, Chem. Mater. 13 (2001) 1213.
[7] Y.D. Yin, X.L. Xu, Chem. Commun. (1998) 1641.
[8] X.F. Qian, X.M. Zhang, C. Wang, Y. Xie, Y.T. Qian, Inorg. Chem. 38 (1999) 2621.
[9] S.H. Yu, L. Shu, J. Yang, Z.H. Han, Y.T. Qian, Y.H. Zhang, J. Mater. Res. 14 (1999) 4157.
[10] S.H. Yu, Y.S. Wu, J. Yang, Z.H. Han, Y. Xie, Y.T. Qian, X.M. Liu, Chem. Mater. 10 (1998) 2309.
[11] H. Wang, J.R. Zhang, J.J. Zhu, J. Crystal Growth 233 (2001) 829.
[12] J.J. Zhu, M.G. Zhou, J.Z. Xu, X.H. Liao, Mater. Lett. 47 (2001) 25.
[13] A.V. Murugan, R.S. Sonawane, B.B. Kale, S.K. Apte, A.V. Kulkarni, Mater. Chem. Phys. 71 (2001) 98.
[14] R.S. Mane, C.D. Lokhande, Mater. Chem. Phys. 65 (2000) 1 and references cited therein..
[15] C.Y. Wang, Y. Zhou, Y.R. Zhu, H.J. Liu, Z.Y. Chen, Mater. Res. Bull. 35 (2000) 1463.
[16] D. Routkevitch, T. Bigioni, M. Moskovits, J.M. Xu, J. Phys. Chem. 100 (1996) 14037.
[17] D.S. Xu, D.P. Chen, Y.J. Xu, X.S. Shi, G.L. Guo, L.L. Gui, Y.Q. Tang, Pure Appl. Chem. 72 (2000) 127.
[18] Y. Mastai, M. Homyonfer, A. Gedanken, Adv. Mater. 11 (1999) 1010.
[19] M.P. Pileni, J. Phys. Chem. 97 (1993) 6961.
[20] V. Pillai, P. Kumar, M.J. Hou, P. Ayyub, D.O. Shah, Adv. Colloid Interface Sci. 55 (1995) 241.

[21] M.J. Schwuger, K. Stickdorn, R. Schomacker, Chem. Rev. 95 (1995) 849.

[22] P. Liaos, J.K. Tomas, J. Colloid Interface Sci. 117 (1987) 506.

[23] R. Vogel, P. Hoyer, H. Weller, J. Phys. Chem. 98 (1994) 3183.

[24] A.R. Kortan, R. Hull, R.L. Opila, M.G. Bawendi, M.L. Steingerwald, P.J. Carrol, L.E. Brus, J. Am. Chem. Soc. 112 (1990) 1327.

[25] S.G. Dixit, A.R. Mahadeshwar, S.K. Haram, Colloids Surf. A 133 (1998) 69.

[26] K.S. Suslick, Ultrasound: Its Chemical, Physical and Biological Effects, VCH, Weinhein, Germany, 1988.

[27] K.S. Suslick, S.B. Choe, A.A. Cichowlas, M.W. Grinstaff, Nature 353 (1991) 414.

[28] M.M. Mdleleni, T. Hyeon, K.S. Suslick, J. Am. Chem. Soc. 120 (1998) 6189.

[29] N. Arul Dhas, A. Zaban, A. Gedanken, Chem. Mater. 11 (1999) 806.

[30] N. Arul Dhas, A. Gedanken, Appl. Phys. Lett. 72 (1998) 2514.

[31] J.J. Zhu, S.W. Liu, O. Palchik, Y. Koltypin, A. Gedanken, J. Solid State Chem. 153 (2000) 342.

[32] R.V. Kumar, O. Palchik, Y. Koltypin, Y. Diamant, A. Gedanken, Ultrasonics Sonochem. 9 (2002) 65.

[33] P. Jeevanandam, Y. Koltypin, Y. Gofer, Y. Diamant, A. Gedanken, J. Mater. Chem. 10 (2000) 2769.

[34] S. Avivi, O. Palchik, V. Palchik, M.A. Slifkin, A.M. Weiss, A. Gedanken, Chem. Mater. 13 (2001) 2195.

[35] G. Wang, G. Li, C. Liang, L. Zhang, Chem. Lett. (2001) 344.

[36] J.Z. Sostaric, R.A. Caruso-Hobson, P. Mulvaney, F. Grieser, J. Chem. Soc. Faraday Trans. 93 (1997) 1791.

[37] J.X. Huang, Y. Xie, B. Li, Y. Liu, J. Lu, Y.T. Qian, J. Colloid Interface Sci. 236 (2001) 382.

[38] M. Sharon, K.S. Ramaiah, M. Kumar, M. Neumann-Spallart, C. Levy-Clement, J. Electroanal. Chem. 436 (1997) 49.

[39] F.C. Meldrum, J. Flath, W. Knoll, J. Mater. Chem. 9 (1999) 711.

[40] R. Thielsch, T. Bohmn, R. Reiche, D. Schlafer, H.D. Bauer, H. Botteher, Nanostruct. Mater. 10 (1998) 131.

[41] H. Klug, L. Alexander, X-ray Diffraction Procedures, Wiley: New York, 1962.

[42] C.D. Wagner, W.M. Riggs, L.E. Davis, J.F. Moulder, B.E. Muilenberg, Handbook of X-ray Photoelectron Spectroscopy, Perkin–Elmer, Physical Electronics Division, Eden Prairie, 1979.

[43] P. Dubois, J.P. Lelieur, G. Lepoutre, Inorg. Chem. 28 (1989) 195.

[44] G. Henshaw, I.P. Parkin, G.A. Shaw, Chem. Commun. (1996) 1095.

[45] G. Henshaw, I.P. Parkin, G.A. Shaw, J. Chem. Soc. Dalton Trans. (1997) 231.

[46] F.A. Cotton, G. Wilkinson, Advanced Inorganic Chemistry, 3rd Edition, Wiley, New York, 1972.

[47] Q.Y. Lu, J.Q. Hu, K.B. Tang, Y.T. Qian, X.M. Liu, G.E. Zhou, J. Solid State Chem. 146 (1999) 484.

[48] K.S. Suslick, D.A. Hammerton, R.E. Cline, J. Am. Chem. Soc. 108 (1986) 5641.

[49] W. Lauterborn, A. Vogel, Annu. Rev., Fluid Mech. 16 (1984) 223.

[50] S. Ramech, Y. Koltypin, A. Gedanken, J. Mater. Res. 12 (1997) 3271.

[51] W. Chen, Z. Wang, Z. Lin, L. Lin, J. Appl. Phys. 82 (1997) 3111.